Overlapping Thin-Section Fast Spin-Echo MR of the Large Vestibular Aqueduct Syndrome

Richard T. Dahlen, H. Ric Harnsberger, Steven D. Gray, Clough Shelton, Robert Allen, James L. Parkin, and David Scalzo

PURPOSE: To evaluate a high-resolution, thin-section fast spin-echo MR imaging technique of the inner ear to identify the large vestibular aqueduct syndrome seen on temporal bone CT scans. **METHODS:** We retrospectively reviewed the temporal bone CT scans of 21 patients with hearing loss and enlarged bony vestibular aqueducts by CT criteria. High-resolution fast spin-echo MR imaging was then performed on these patients using dual 3-inch phased-array receiver coils fixed in a temporomandibular joint holder and centered over the temporal bones. MR imaging included axial and oblique sagittal fast spin-echo sequences. The diameter of the midvestibular aqueduct on CT scans and the signal at the level of the midaqueduct on MR images were measured on axial sequences, then compared. High-resolution MR imaging with the same protocol was performed in 44 control subjects with normal ears, and similar measurements were taken. **RESULTS:** The average size of the enlarged bony vestibular aqueduct on CT scans was 3.7 mm, and the average width of the signal from within the enlarged aqueduct on MR images was 3.8 mm. Statistical analysis showed excellent correlation. MR images alone displayed the enlarged extraosseous endolymphatic sac, which accompanies the enlarged aqueduct in this syndrome. Five ears in three patients with enlarged bony vestibular aqueducts on CT scans showed no evidence of an enlarged endolymphatic duct or sac on MR images. An enlarged endolymphatic sac was seen on MR images in one patient with a bony vestibular aqueduct, which had normal measurements on CT scans. MR imaging alone identified a single case of mild cochlear dysplasia (Mondini malformation). In the 88 normal ears studied, the average size of the endolymphatic sac at its midpoint between the common crus and the external aperture measured on MR images was 0.8 mm (range, 0.5 to 1.4 mm). In 25% of the normal ears, no signal was seen from within the vestibular aqueduct. **CONCLUSION:** Thin-section, high-resolution fast spin-echo MR imaging of the inner ear is complementary to CT in studying patients with the large vestibular aqueduct syndrome, as MR imaging better displays the soft tissues and fluid of the membranous labyrinth.

Index terms: Ear, abnormalities and anomalies; Ear, magnetic resonance

AJNR Am J Neuroradiol 18:67–75, January 1997

High-resolution thin-section computed tomography (CT) has been the mainstay of inner ear imaging because of its high spatial resolution and contrast (1–3). In the past, magnetic resonance (MR) imaging of the inner ear has had a limited role owing to problems with signal loss from local field inhomogeneities produced from the juxtaposition of dense temporal bone, otic capsule, and pneumatized air cells. Initial attempts to obtain high-resolution images of the temporal bone relied on gradient-echo techniques (4–9). Gradient-echo sequences are inherently sensitive to the magnetic susceptibility artifacts produced by the air-bone interfaces found within the temporal bone. As a result, early attempts to produce consistently diagnostic images of the temporal bone with MR imaging were variably successful, and CT has re-

Received December 6, 1995; accepted after revision June 13, 1996.

Dr Dahlen was the recipient of the Head and Neck Radiologist in Training Award at the 1995 meeting of the American Society of Head and Neck Radiology in Pittsburgh, Pa.

From the Departments of Radiology (R.T.D., H.R.H., R.W.A., D.S., K.T.) and Surgery, Division of Otolaryngology-Head and Neck Surgery (S.D.G., C.S., J.L.P.), University of Utah Health Sciences Center, Salt Lake City.

Address reprint requests to H. Ric Harnsberger, MD, Department of Radiology, University of Utah Health Sciences Center, 50 N Medical Dr, Salt Lake City, UT 84132.

AJNR 18:67–75, Jan 1997 0195-6108/97/1801–0067

mained the technique of choice in the radiologic evaluation of congenital inner ear anomalies (10).

Fast spin-echo pulse sequences are inherently less sensitive to magnetic susceptibility signal loss while being capable of producing high-resolution T2-weighted images (7, 8). Consequently, fast spin-echo techniques are ideally suited for temporal bone imaging. The time savings gained through the use of a greater echo train length with fast spin-echo can be translated into increased spatial resolution by increasing the matrix and/or the number of averages (10).

The normal endolymphatic duct originates in the anteromedial wall of the vestibule, coursing posterolaterally in the bony vestibular aqueduct to merge with the endolymphatic sac while remaining within the bony canal. The endolymphatic sac then emerges from the bony vestibular aqueduct in a shallow impression on the posterior face of the petrous temporal bone (11–14) (Fig 1A). The function of the endolymphatic duct and sac is not well understood. Endolymph produced in the cochlea travels from the inner ear to the endolymphatic sac. The endolymphatic sac functions as a metabolically active filter to regulate the volume and composition of the endolymphatic fluid. Loss of function of the endolymphatic sac or abnormalities in this region have been implicated in Meniere disease (13).

The large vestibular aqueduct syndrome is thought to be a result of arrest of the normal development of the endolymphatic duct and sac (2, 3, 15, 16). Instead of the normal inverted J shape, the duct and sac remain enlarged in their early embryological form (Fig 1B). Patients with this congenital anomaly typically have some hearing at birth but progressively lose this hearing in the first years of life (1, 2, 15, 17).

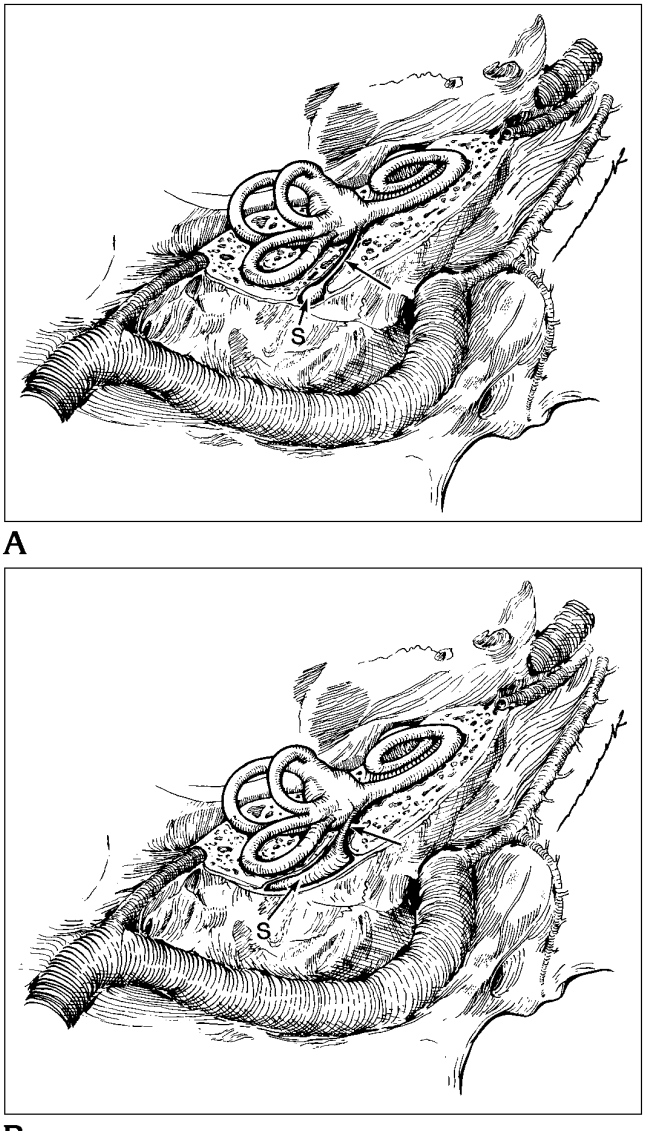

Fig 1. *A*, The anatomy of the normal right inner ear, viewed from above and behind the temporal bone. The endolymphatic duct (*arrow*) courses through the proximal bony vestibular aqueduct from its internal aperture in the anteromedial wall of the vestibule to the endolymphatic sac (*S*) found in the bony aqueduct and within a shallow impression on the posterior face of the petrous temporal bone.

B, Drawing from the same vantage point as in *A* depicts an enlarged right endolymphatic duct and sac. The endolymphatic duct (*arrow*) and the bony channel through which it courses (vestibular aqueduct) are enlarged. The endolymphatic sac (*S*), which lies within the distal aqueduct and between the leaves of the dura along the posterior aspect of the petrous pyramid, is also enlarged.

Subjects and Methods

We first determined the normal diameter range for the midlevel endolymphatic sac on high-resolution MR images by measuring the width of signal at the level of the vestibular aqueduct in 44 healthy volunteers (88 normal inner ears) after obtaining informed consent. These subjects underwent high-resolution fast spin-echo MR imaging on a 1.5-T superconducting MR unit. A dual, 3-inch phased-array receiver coil fixed in a temporomandibular joint holder and centered over the temporal bones was used. Imaging included a coronal fast spin-echo localizer se-

quence followed by axial and oblique sagittal (parallel to the turns of the cochlea) sequences. Imaging parameters were 4000/90/6 (repetition time/effective echo time/excitations), an echo train length of 32, a 512 × 512 matrix, a 20 × 10 field of view, and 2-mm-thick sections with 1-mm overlap. A triple acquisition was used to eliminate saturation and minimize crosstalk. The approximate imaging times were 9 minutes for the axial sequence and 7 minutes for the oblique sagittal sequence. The membranous contents of the vestibular aqueduct (endolymphatic duct and sac) were measured at the midportion of the canal between the common crus and the external aperture using a calibrated jeweler's eyepiece. This measurement location has been used previously for CT measurements of the bony vestibular aqueduct (2). In addition, the healthy volunteers were examined for the presence of a visible extraosseous endolymphatic sac on high-resolution MR images.

In the second phase of the study, we compared high-resolution, thin-section fast spin-echo MR images with CT scans obtained in patients with enlarged bony vestibular aqueducts. First, thin-section temporal bone CT scans of 21 patients with unilateral or bilateral hearing loss and unilateral or bilateral enlarged bony vestibular aqueducts were reviewed retrospectively. We then examined these patients with high-resolution fast spin-echo MR imaging of the temporal bones using a technique identical to that used with the volunteer subjects. All CT scans were viewed at a window setting of 4000 and a level setting of 450. Eight of the CT studies were performed with 1.5-mm axial sections and 13 with 1-mm axial sections. All MR imaging window and level settings were adjusted to maximize detail of the cochlear contents.

The diameter of the bony vestibular aqueduct was measured on CT scans at its midpoint between the common crus and the external aperture using a calibrated jeweler's eyepiece. As described by Valvassori (15, 17), a measurement greater than 1.5 mm was considered enlarged. This value is consistent with that used in a microdissection study of human temporal bones reported by Wilbrand et al (18), in which the normal diameter of the vestibular aqueduct ranged from 0.4 to 1.0 mm. The contents of the vestibular aqueduct were measured in an identical manner and location on the axial fast spin-echo MR images. The measurements obtained on the CT and MR studies were compared using a regression coefficient. The CT and MR examinations were also evaluated for the morphology of the vestibule, cochlea, semicircular canals, and endolymphatic sac. The size of the endolymphatic sac was measured using a calibrated jeweler's eyepiece.

Complete audiometric data were available for 11 patients. Clinical records were reviewed for the age of onset of hearing loss, progression of hearing loss, unilateral or bilateral hearing loss, and precipitating events for hearing loss. The structural abnormalities observed were compared with the degree and laterality of the hearing loss in those patients for whom audiometric data were available.

Results

The control group consisted of 44 healthy subjects, 26 male and 18 female, 8 to 73 years old (average age, 43 years), in whom 88 ears were examined with high-resolution, thin-section fast spin-echo MR imaging. In 22 (25%) of the 88 inner ears imaged, an endolymphatic duct or sac could not be identified, despite high-resolution images without motion artifacts. In those ears in which the sac was identified, the diameter ranged from 0.5 to 1.4 mm (average, 0.8 mm) when measured at its midportion (Fig 2). The morphology of the vestibule, cochlea, and semicircular canals was normal in all control subjects. The extraosseous endolymphatic sac along the posterior aspect of the temporal bone could not be identified in any of the control subjects.

The group with large bony vestibular aqueducts on CT scans consisted of 12 females and nine males. The average age was 17 years (range, 1 to 49 years); eight patients were older than 18 years.

On temporal bone CT scans, all patients had at least one enlarged vestibular aqueduct (>1.5 mm in diameter). Seventeen patients had bilateral and four patients had unilateral enlarged bony vestibular aqueducts (38 ears total) (Figs 3 and 4). The minimum midaqueduct diameter was 1.7 mm, the maximum was 6.8 mm (average, 3.7 mm).

The fast spin-echo MR images in this group with abnormal CT findings revealed a large endolymphatic sac (>1.5 in mm) in all but three patients (five ears). In these three patients, no enlargement of the endolymphatic system was seen on the MR images (Fig 5). Sixteen patients had bilateral and two patients had unilateral enlarged vestibular aqueducts on MR images. In one patient with bilateral hearing loss who appeared to have a unilateral enlarged vestibular aqueduct on CT scans, bilateral enlarged endolymphatic ducts and sacs were seen on MR images (Fig 6). The minimum midaqueduct diameter was 2.1 mm, the maximum was 7.2 mm (average, 3.8 mm) on the MR images.

Bilateral cochlear dysplasias were seen in four patients with CT evidence of a large bony vestibular aqueduct. All these cochlear abnormalities were identified on the MR images. In addition, one patient with a unilateral enlarged vestibular aqueduct on CT scans was also found to have a subtle cochlear dysplasia only on MR

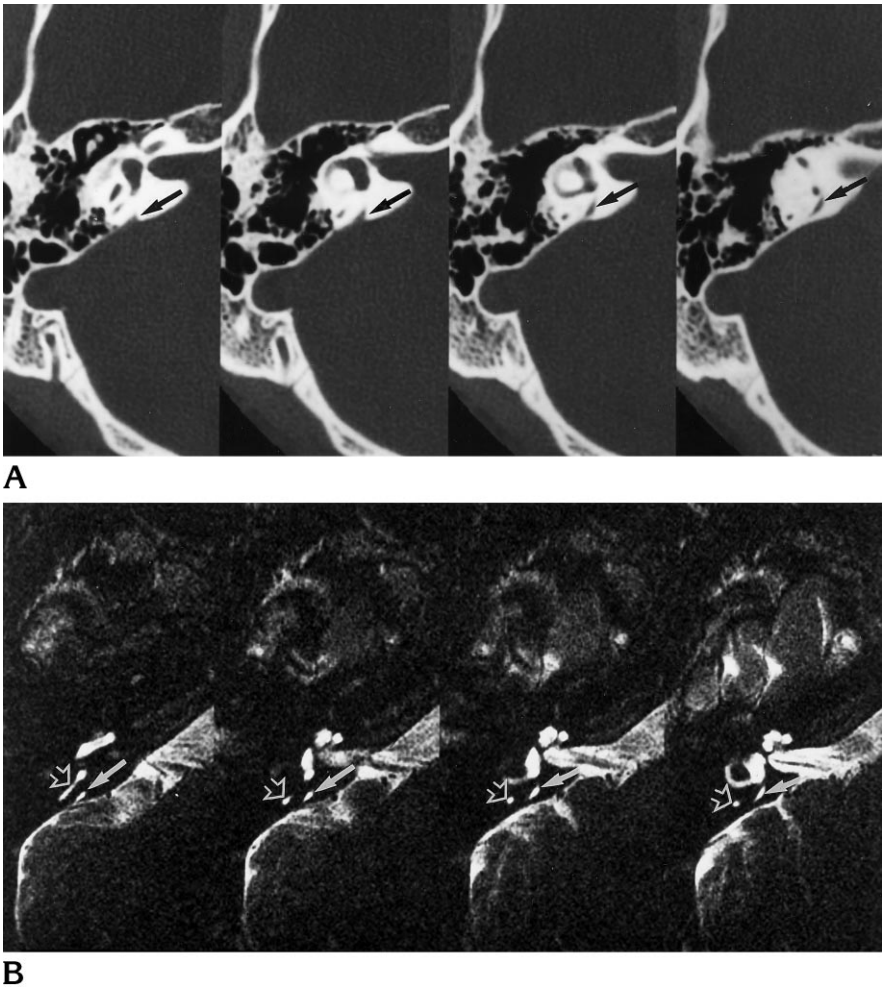

Fig 2. *A*, Temporal bone axial CT scans show normal vestibular aqueduct. This bony vestibular aqueduct (*arrows*), while prominent, is normal in size (less than 1.5 mm).

B, Normal endolymphatic sac on fast spin-echo MR images. On axial high-resolution T2-weighted fast spin-echo MR images, the endolymphatic sac (*solid arrows*) is seen in the same patient as in *A*. The position is parallel to the posterior semicircular canal (*open arrows*) and just posterior to it.

images (Fig 7). Three patients had bilateral and one patient had unilateral cystic dysplasia of the vestibule on CT scans. These were all seen on the fast spin-echo MR images. Three cases of bilateral cystic dysplasia of at least one semicircular canal were evident on CT scans. All these were seen on the fast spin-echo MR images. There were no additional cases of cystic vestibule or semicircular canals on MR images that were not seen on CT scans.

Audiometric data were available for 11 patients, representing 21 ears with hearing loss. The hearing loss was profound (>80 dB) in 14, severe (60 to 80 dB) in three, moderate (50 to 59 dB) in three, and mild (30 to 49 dB) in one. The hearing loss was a down-sloping predominately high-frequency loss in 20 patients and a uniform loss at all frequencies in one patient. The age of onset of hearing loss was available in 13 patients. Six patients had hearing loss since birth, two patients had loss at 3 years of age, and one patient each had loss at 2, 4, 8, 17, and 45 years of age.

The side with the largest endolymphatic sac on MR images corresponded to the side with the greatest hearing loss in eight of 10 patients in whom bilateral large vestibular aqueduct syndrome and audiometric data were available. The remaining two patients had profound bilateral hearing loss. However, when the size of the endolymphatic duct or sac was compared with the degree of hearing loss, no correlation appeared to exist.

In two patients, the onset of hearing loss was precipitated by trauma. One 17-year-old girl had stepwise progression of hearing loss after two motor vehicle accidents. A 45-year-old woman first experienced hearing loss after a heavy object fell on her head.

The direct axial images were the most useful for examining the endolymphatic duct and sac. The oblique sagittal images parallel to the co-

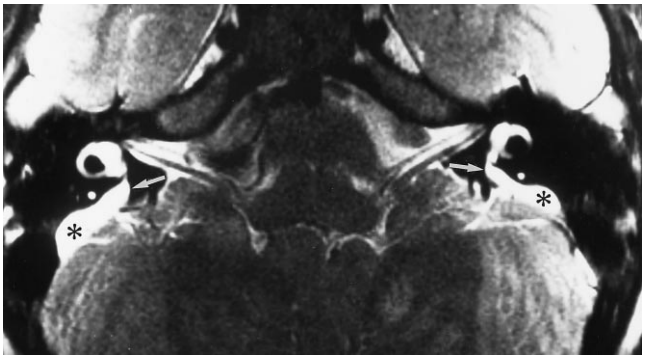

Fig 3. Axial fast spin-echo MR image of bilateral enlarged endolymphatic ducts and sacs. In this patient, the bilateral endolymphatic ducts (*arrows*) are enlarged (>1.5 mm in diameter). Also seen are enlarged endolymphatic sacs (*asterisks*).

chlear turns were helpful for determining cochlear dysplasia.

Discussion

The radiologic description of the large vestibular aqueduct syndrome was defined by Valvassori using polytomography in 1978 (17). The large bony vestibular aqueduct was further measured and defined with the use of CT during subsequent years (1, 3). Gradient-echo MR imaging followed, allowing the first radiologic look at both the endolymphatic duct and sac (4, 7). Susceptibility artifacts associated with gradient-echo techniques of the inner ear hampered the evolution of MR imaging in examining patients with congenital hearing loss. With the arrival of fast spin-echo pulse sequences, high-resolution MR imaging of the inner ear unaffected by significant signal loss from susceptibility artifacts became available (10). In this study, we compared high-resolution fast spin-echo MR imaging with temporal bone CT in patients with CT-proved large vestibular aqueduct syndrome in an attempt to evaluate the usefulness of MR imaging in this patient population.

With fast spin-echo MR imaging, as with any new imaging technique, determining what is normal versus abnormal is critical to radiologic interpretation. The average normal midpoint diameter (0.8 mm) and range (0.5 to 1.4 mm) of the transverse endolymphatic sac measured on fast spin-echo MR images in this study correspond well to values reported in the literature. On polytomographic studies, Becker et al (19) found a maximal normal diameter of 1.25 mm, while Kraus and Dubois (20) reported a mean diameter of 0.8 mm with a range of 0.1 to 2.0

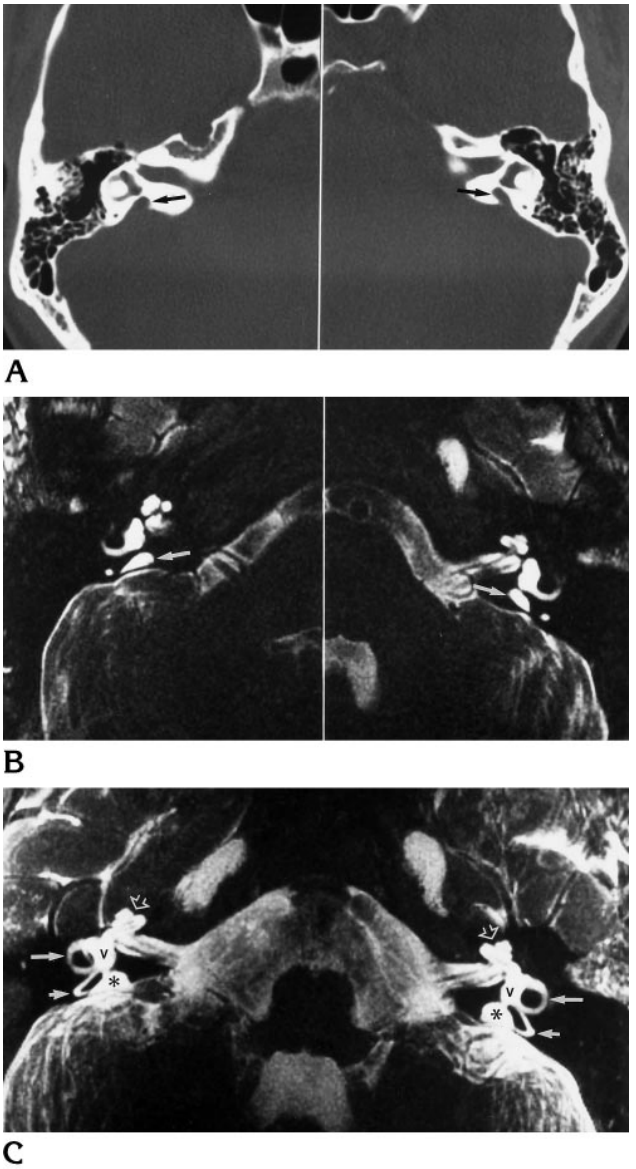

Fig 4. Bilateral enlarged endolymphatic ducts and sacs.

A, The bony vestibular aqueduct (*arrows*) is enlarged on axial CT scans.

B, Axial fast spin-echo MR images show enlarged endolymphatic sacs (*arrows*).

C, Axial maximum intensity projection fast spin-echo MR image reveals the membranous labyrinth anatomy: cochlea (*open arrows*), vestibule (*V*), horizontal semicircular canal (*long solid arrows*), posterior semicircular canal (*short solid arrows*), enlarged endolymphatic duct and sac (*asterisk*).

mm measured transversely at the midpoint of the posterior limb of the vestibular aqueduct. In the majority of CT studies, investigators considered a bony vestibular aqueduct enlarged if its diameter was greater than 1.5 to 2.0 mm (2, 3, 15, 21). None of our measurements in normal ears exceeded this range. Finally, in a microdissection study of human temporal bones, Wil-

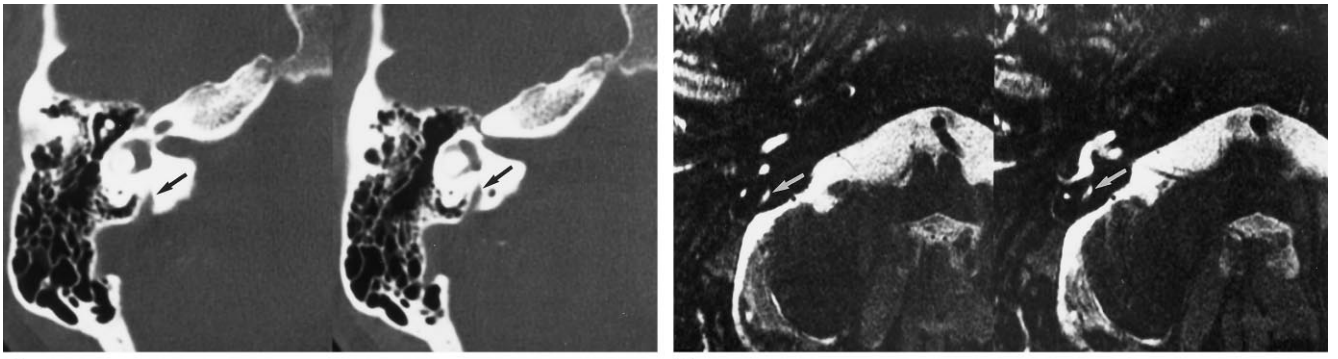

A B

Fig 5. Enlarged bony vestibular aqueduct on temporal bone CT with normal findings at MR imaging.

A, On axial temporal bone CT scans of the right ear, the vestibular aqueduct is enlarged (*arrow*), measuring 2.4 mm at the transverse midpoint.

B, Axial fast spin-echo MR images show a normal-appearing endolymphatic sac (*arrow*), which measures 1.3 mm at its transverse midpoint.

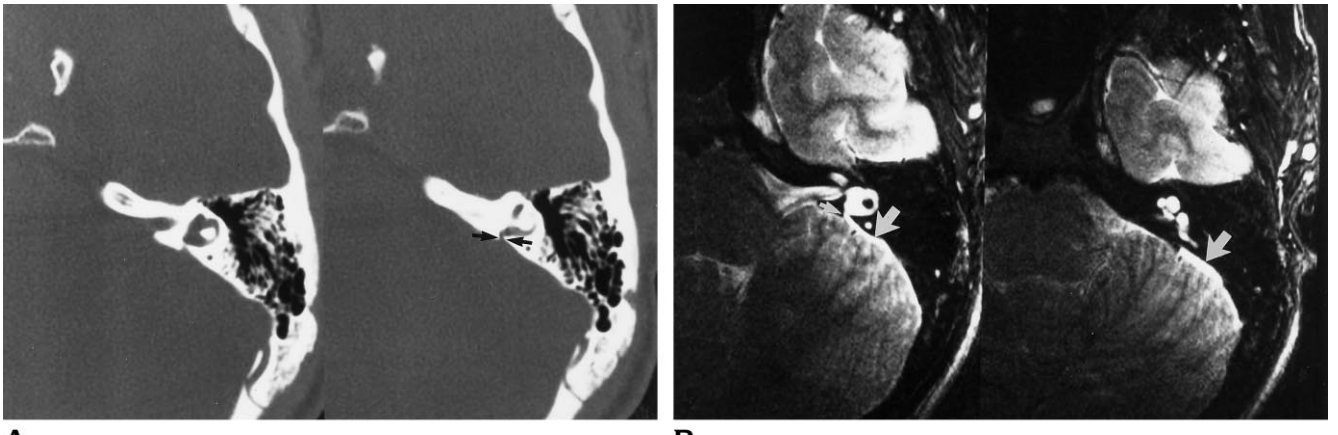

A B

Fig 6. Prominent vestibular aqueduct that is indeterminate on CT but enlarged at MR imaging.

A, Axial CT scans show the bony vestibular aqueduct (*arrows*) as slightly enlarged, but it is difficult to measure, owing to the unusual appearance of the posterior margin of the temporal bone. There is a very short distance between the vestibule and the posterior temporal bone, making it difficult to measure accurately the vestibular aqueduct, which is very short.

B, On axial fast spin-echo MR images, the endolymphatic duct (*small arrow*) is enlarged (2.1 mm) and is associated with an enlarged endolymphatic sac (*large arrow*). Direct visibility of the membranous contents of the vestibular aqueduct and the presence of an enlarged endolymphatic sac make the abnormality easier to appreciate.

brand et al (18) found a normal diameter range of 0.4 to 1.0 mm for the midpoint transverse bony vestibular aqueduct. On the basis of these comparisons, we concluded that any transverse measurement under 1.5 mm at the level of the midpoint of the vestibular aqueduct on fast spin-echo MR images is normal. Note that in 25% of our healthy subjects, the endolymphatic duct and sac could not be seen; thus, nonvisibility need not be pathologic.

In the group with abnormal findings, the average transverse midpoint diameter of the bony vestibular aqueduct on CT scans (3.7 mm) and the similarly measured diameter of the endolymphatic sac on fast spin-echo MR images (3.8 mm) were similar, with a correlation coefficient of $r^2 = .96$. However, when the individual values are examined, the transverse midpoint diameter on MR images was consistently minimally larger than that on CT scans. A paired t test revealed a significant difference ($P = .04$). A "blooming effect" of the bright endolymph, causing a slight increase in the measurement on MR images in each case, may explain this small discrepancy. Window and level settings on MR images may also be a contributing factor.

At first glance, comparing a healthy control population with an average age of 43 years with a study group whose average age was 17 years may seem incorrect. However, Kodama and

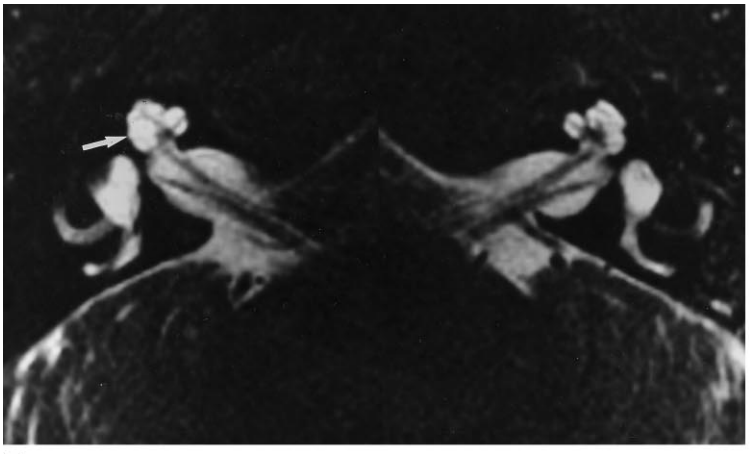

7

Fig 7. Subtle cochlear dysplasia is seen on this axial fast spin-echo MR image as a small cystic region within the cochlea (*arrow*), which was not visible on temporal bone CT scans. The opposite, normal, side shows the normal cochlear morphology for comparison.

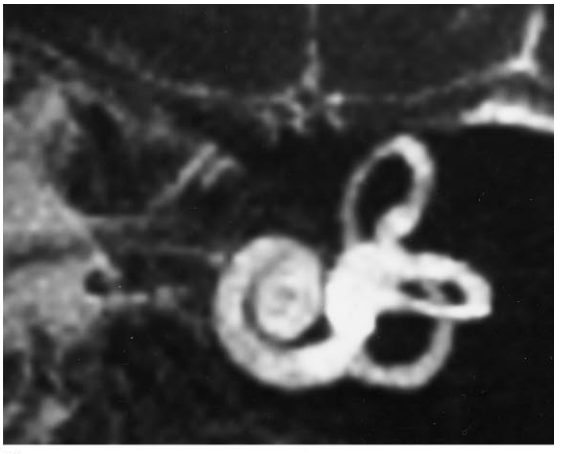

8

Fig 8. Oblique sagittal maximum intensity projection image constructed from the thin-section T2-weighted fast spin-echo MR source images gives a three-dimensional appearance to this normal inner ear.

Sando (14), in a study of the diameter of the bony vestibular aqueduct in human temporal bones of persons 0 to 13 years old, concluded that the bony vestibular aqueduct and the rugose portion of the endolymphatic sac increase slowly in size from birth until 3 years of age, at which point adult size is obtained and no further change in size is seen. Given the stability of size after the first 3 years of life, we felt justified in using our comparison population despite the age difference.

In the majority of ears with enlarged vestibular aqueducts on CT scans, a corresponding enlarged endolymphatic sac was seen on MR images (34 on MR images, 38 on CT scans). Two circumstances in which the two studies did not agree were when the CT measurement suggested the diagnosis of large vestibular aqueduct syndrome but fast spin-echo MR images showed a normal endolymphatic sac, and when the CT measurement of the vestibular aqueduct was normal but fast spin-echo MR images showed an enlarged endolymphatic sac. Three patients (five ears) had large bony vestibular aqueducts measured on CT scans with fast spin-echo MR images that showed a normally sized endolymphatic duct and sac (Fig 5). The direct visibility with MR imaging of the fluids and soft tissues of the membranous labyrinth that were normal in these cases might suggest that the CT scan produced a false-positive finding. However, the presence of hearing loss involving these ears and the enlarged vestibular aqueduct on CT scans would suggest a true-positive result. Without a standard of reference it is difficult to ascertain which test is correct. One possibility to explain the positive CT and negative MR result is prior enlargement of the endolymphatic duct and sac with associated enlargement of the bony vestibular aqueduct. If for some reason the pliable endolymphatic duct and sac returned to normal size, the bony vestibular aqueduct would remain enlarged, resulting in the positive CT finding.

A second advantage of fast spin-echo MR imaging is exemplified in one patient in whom CT scans showed a unilateral large bony vestibular aqueduct while fast spin-echo MR images revealed bilateral enlarged endolymphatic ducts and sacs (Fig 6). If CT alone had been performed in this patient, this congenital anomaly would have only been diagnosed in one ear, with the other ear considered radiologically normal. Fast spin-echo MR imaging clearly defined an abnormal sac in the ear that appeared normal on CT scans. In this case, the posterior wall of the vestibular aqueduct was short, so most of the sac was extraosseous. Because only the extraosseous segment was enlarged, the abnormality was visible with MR imaging but not with CT. Although this false-negative CT finding was seen only once in this small series, it suggests that congenital anomalies may be missed by CT alone. A second case in this study in which CT

showed a normal cochlea but MR imaging displayed a mild cochlear dysplasia (Fig 7) substantiates the premise that fast spin-echo MR imaging is a complementary radiologic tool in this clinical setting.

Fast spin-echo MR imaging alone showed the size and extent of the endolymphatic sac in the group of patients with an enlarged vestibular aqueduct. The endolymphatic sac on T2-weighted fast spin-echo MR images appears as a focal collection of CSF-intensity fluid that communicates directly with the endolymphatic duct. CT of the temporal bone did not show the extraosseous endolymphatic sac in any of these cases because of its location outside the confines of the temporal bone itself. A larger field of view on CT scanning with soft-tissue windows would reveal the endolymphatic sac as an enlarged CSF space along the posterior temporal bone. However, such scans are not routinely obtained. All patients who had an enlarged intraosseous sac on fast spin-echo MR images also had an enlarged extraosseous sac, which agrees with previous reports on this subject (1, 2, 12, 14, 22). The smallest endolymphatic sac in our series associated with a large endolymphatic duct measured 2 $\times$ 6 mm; the largest was 9 $\times$ 19 mm, with average sac size of 5 $\times$ 13 mm as measured in the greatest dimension in the axial plane. Microsurgical analysis in the healthy adult shows a mean width and height of the sac to be 3.83 mm and 3.80 mm, respectively (23). Enlargement of the endolymphatic sac on fast spin-echo MR images in this study was bilateral in 89% of patients, compared with values reported in the literature that range from 60% to 94% (1, 2, 15, 21).

Of the 34 ears with enlarged endolymphatic sacs by fast spin-echo MR imaging, 27% had an abnormal cochlea, 31% had a cystic vestibule, and 23% had abnormal semicircular canals. Bilateral cochlear dysplasias were seen in four of the patients with a large endolymphatic sac. All dysplasias were of the incomplete partition type, as described by Jackler et al (16), in which the basal turn is formed normally but the apical turn is abnormal.

In summary, fast spin-echo MR imaging can directly show the fluid spaces and soft tissues of the membranous labyrinth. Temporal bone CT, on the other hand, best delineates the bony labyrinth, conveying soft-tissue information by inference only. Thin-section, high-resolution fast spin-echo MR images of the inner ear provide adequate detail of the fluid and soft-tissue contents of the aqueduct to diagnose the large vestibular aqueduct syndrome confidently. An additional advantage of this thin-section fast spin-echo MR technique is the presence of adequate source image data, which can be subjected to a postprocessing maximum intensity projection algorithm, creating a unique dimensional sense that may be of help in further fining congenital inner ear malformations (Fig 8).

References

1. Levenson MJ, Parisier SC, Morton J, Edelstein DR. The large vestibular aqueduct syndrome in children. *Arch Otolaryngol Head Neck Surg* 1989;115:54–58
2. Jackler RK, De La Cruz A. The large vestibular aqueduct syndrome. *Laryngoscope* 1989;99:1238–1243
3. Urman SM, Talbot JM. Otic capsule dysplasia: clinical and CT findings. *Radiographics* 1990;10:823–838
4. Brogan MA, Chakeres DW, Schmalbrock P. High-resolution 3DFT MR imaging of the endolymphatic duct and soft tissues of the otic capsule. *AJNR Am J Neuroradiol* 1991;12:1–11
5. Schmalbrock P, Brogan MA, Chakeres DW, et al. Optimization of submillimeter resolution MR imaging methods for the inner ear. *J Magn Reson Imaging* 1993;3:451–459
6. Casselman JW, Kuhweide R, Deimling M, et al. Constructive interference in steady state 3DFT MR imaging of the inner ear and cerebellopontine angle. *AJNR Am J Neuroradiol* 1993;14:47–57
7. Casselman JW, Kuhweide R, Ampe W, et al. Pathology of the membranous labyrinth: comparison of T1- and T2-weighted and gadolinium-enhanced spin-echo and 3DFT-CISS imaging. *AJNR Am J Neuroradiol* 1993;14:59–69
8. Casselman JW, Majoor MHJM, Albers FW. MR of the inner ear in patients with Cogan syndrome. *AJNR Am J Neuroradiol* 1994;15: 131–138
9. Harnsberger HR, Dart DJ, Parkin JL, et al. Cochlear implant candidates: assessment with CT and MR imaging. *Radiology* 1987; 164:53–57
10. Tien RD, Felsberg GJ, Macfall J. Fast spin-echo high-resolution MR imaging of the inner ear. *AJR Am J Roentgenol* 1992;159: 395–398
11. Schuknecht HF. *Pathology of the Ear*. 2nd ed. Philadelphia, Pa: Lea & Febiger; 1993:61–62
12. Ogura Y, Clemis JD. A study of the gross anatomy of the human vestibular aqueduct. *Ann Otol* 1971;80:813–825
13. Schuknecht HF. *Pathology of the Ear*. 2nd ed. Philadelphia, Pa: Lea & Febiger; 1993:103–105
14. Kodama A, Sando I. Postnatal development of the vestibular aqueduct and endolymphatic sac. *Ann Otol Rhinol Laryngol* 1982;91(suppl 96):3–12
15. Valvassori GE. The large vestibular aqueduct and associated anomalies of the inner ear. *Otolaryngol Clin North Am* 1983;16: 95–101
16. Jackler RK, Luxford WM, House WF. Congenital malformations of the inner ear: a classification based on embryogenesis. *Laryngoscope* 1987;97(part 2, suppl 40):2–14
17. Valvassori GE, Clemis JD. The large vestibular aqueduct syndrome. *Laryngoscope* 1978;88:723–728
18. Wilbrand HF, Rask-Anderson H, Gilstring D. The vestibular aque-

duct and paravestibular canal: an anatomic and radiologic investigation. *Acta Radiol (Diagn)* 1974;15:337–355
19. Becker TS, Vignaud J, Sultan A. The vestibular aqueduct in congenital deafness: evaluation by the axial projection. *Radiology* 1983;149:741–744
20. Kraus EM, Dubois PJ. Tomography of the vestibular aqueduct in ear disease. *Arch Otolaryngol* 1979;105:91–98
21. Emmett JR. The large vestibular aqueduct syndrome. *Am J Otol* 1985;6:387–415
22. Gussen R. The endolymphatic sac in the Mondini disorder. *Arch Otorhinolaryngol* 1985;242:71–76
23. Ammirati M, Aldo S, Feghali J, et al. The endolymphatic sac: microsurgical topographic anatomy. *Neurosurgery* 1995;36:416–418